

II.C.1 High Efficiency Solar Thermochemical Reactor for Hydrogen Production

Anthony McDaniel
Sandia National Laboratories
MS9052
P.O. Box 969
Livermore, CA 94550
Phone: (925) 294-1440
Email: amcdani@sandia.gov

DOE Manager
Katie Randolph
Phone: (720) 356-1759
Email: Katie.Randolph@ee.doe.gov

Subcontractors:

- Profs. Ellen Stechel and Nathan Johnson, Arizona State University, Tempe, AZ
- Prof. Nathan Siegel, Bucknell University, Lewisburg, PA
- Prof. Ryan O'Hayre and Dr. Jianhua Tong, Colorado School of Mines, Golden, CO
- Prof. Christopher Wolverton, Northwestern University, Evanston, IL
- Prof. William Chueh, Stanford University, Stanford, CA

Project Start Date: October 1, 2014
Project End Date: September 30, 2016

Overall Objectives

- Verify the potential for solar thermochemical cycles for hydrogen production to be competitive in the long-term and by 2020, develop this technology to produce hydrogen with a projected cost of \$3.00/gge (gasoline gallon equivalent) at the plant gate
- Develop a high-efficiency particle bed reactor for producing hydrogen via a thermochemical water-splitting cycle, and demonstrate eight continuous hours of operation on a solar simulator producing greater than 3 liters of hydrogen

Fiscal Year (FY) 2015 Objectives

- Discover and characterize suitable materials for two-step, non-volatile metal oxide thermochemical water-splitting cycles
- Design a particle receiver-reactor capable of continuous operation at 3 kW thermal input
- Develop a detailed unit operations model of a large scale single tower, multiple receiver solar thermochemical reactor

Technical Barriers

This project addresses the following technical barriers from the Hydrogen Production section of the Fuel Cell Technologies Office Multi-Year Research, Development, and Demonstration Plan:

- (S) High-Temperature Robust Materials
- (T) Coupling Concentrated Solar Energy and Thermochemical Cycles
- (X) Chemical Reactor Development and Capital Costs
- (AC) Solar Receiver and Reactor Interface Development

Technical Targets

This project is conducting fundamental studies on materials for use in concentrated solar power applications and designing reactor concepts that, when combined, will produce H₂ from thermochemical water-splitting (WS) cycles. Insights gained from these studies will be applied toward the design and optimization of a large-scale solar receiver and reactor that meets the following ultimate DOE hydrogen production targets:

- Hydrogen Cost: <\$2/kg H₂
- Material of Reaction Cost: ≤\$11,000/yr-TPD (metric tons per day) H₂
- Solar-to-Hydrogen (STH) Conversion Ratio: ≥26%
- 1-Sun Hydrogen Production Rate: ≥2.1×10⁻⁶ kg/s m²

FY 2015 Accomplishments

- Extended approach to material development by exploring several doped transition metal redox couples, streamlining screening experiments, and using first principles theory to inform discovery
- Used component-level modeling to establish design criteria for a 3 kW prototype reactor, developed conceptual layout of reactor, and derived hardware solutions for the solar-particle interface, pumping of reduction chambers, pressure separation, and particle flow
- Assembled and tested Olds Lift™ particle elevator, and qualified particle conveyance rates and vacuum separation



INTRODUCTION

This research and development project is focused on the advancement of a technology that produces hydrogen at a cost that is competitive with fossil-based fuels for transportation. A two-step, solar-driven WS thermochemical cycle is theoretically capable of achieving a STH conversion ratio that exceeds the DOE target of 26% at a scale large enough to support an industrialized economy [1]. The challenge is to transition this technology from the laboratory to the marketplace and produce H₂ at a cost that meets or exceeds the DOE target of <\$2/kg H₂.

Conceptually, heat derived from concentrated solar energy can be used to reduce a metal oxide at high temperature producing O₂ (step 1). The reduced metal oxide is then taken “off sun” and re-oxidized at lower temperature by exposure to H₂O, thus producing H₂ (step 2) and completing the cycle. Commercial success of solar thermochemical H₂ production is contingent upon developing suitable redox active materials and incorporating them into an efficient reactor. There are numerous material chemistries that have attributes suitable for inclusion in a thermochemical H₂ production system [2–4]. The challenge is to identify an optimally performing material. In addition, the development of redox material and reactor are not mutually exclusive, but must be conducted in parallel [5]. To maximize the probability of success, this project also addresses the reactor- and system-level challenges related to the design of an efficient particle-based reactor concept [6].

APPROACH

Thermochemical WS reactors are heat engines that convert concentrated solar energy (heat) to chemical work. Our approach is to discover materials to accomplish the WS chemistry and pair these materials with a novel cascading pressure receiver reactor (CPR2) that, when combined, can achieve an unprecedented STH conversion ratio. The material discovery work involves expanding our understanding of the underlying thermodynamics and kinetics in order to make performance improvements and/or formulate new, more redox-active compositions. Sandia’s patented CPR2 technology is based on a moving bed of packed particles that embodies key design attributes essential for achieving high efficiency operation: (1) sensible heat recovery; (2) spatial separation of pressure, temperature, and reaction products; (3) continuous on sun operation; and (4) direct absorption of solar radiation by the redox-active material. Research efforts are focused on demonstrating this technology in a 3 kW-scale prototype.

RESULTS

Materials Research and Development Thrust

Sandia and collaborators synthesized and screened a select group of compounds for redox and WS activity. The synthesis effort was guided by experience gained through two years of investigating perovskite-type oxides for two-step thermochemical WS cycles. We also began two research initiatives, (1) application of first principles theory to inform the material discovery effort and (2) hypothesis testing of concepts for engineering the reduction entropy of WS materials (not discussed herein).

Seventy different compounds representing 14 perovskite families, and a LAMOX and a zircon-type crystal structure, were synthesized from 13 elements (Al, Ca, Ce, Fe, La, Mn, Mo, Nb, O, Sr, Ti, V, and Zr) in nine months of this project year. The Ce^{3+/4+}, Fe^{3+/4+}, Mn^{3+/4+}, Mo^{3+/4+}, Ti^{3+/4+}, and V^{4+/5+} redox couples were explored. We adopted a more efficient primary screening methodology, called temperature programmed reaction (TPR), using a thermogravimetric analyzer (TGA) in order to keep pace with the synthesis activity. This approach measures oxygen evolution behavior during a single heat cycle and then infers WS candidacy from two figures of merit: (1) a redox capacity that exceeds CeO₂ (0.01 mol O/mol sample) and (2) an onset temperature for oxygen release (T_{OR}) between SLMA6464 (850°C) and CeO₂ (1220°C). While this method is currently deployed on a TGA, primary screening experiments can also run on conventional flow reactors if necessary to increase throughput.

Shown in Figure 1a are mass loss TPR profiles for representative materials from each group of the aforementioned compounds compared to CeO₂. From this data the T_{OR} can be derived, as shown in Figure 1b. The maximum reduction capacity is specified by the negative numbers inset to graph in Figure 1a, with more negative values indicating greater capacity. It is clear from this dataset that all compounds screened thus far have a greater redox capacity than CeO₂ under the conditions of this experiment. It is also clear that a few compounds, namely those with T_{OR} between SLMA6464 and CeO₂, are possible candidates for WS. We are most encouraged by COMP X, which is currently undergoing detailed analysis at Sandia’s stagnation flow reactor (SFR) [7] facility.

While we have high confidence in our chemical intuition, the number of possible WS materials thought to exist within the perovskite family alone is extremely large. Therefore, we initiated a computational screening methodology, based on density functional theory (DFT), to inform the discovery effort. Two of the most challenging aspects of DFT are gaining confidence in the applicability of available pseudopotentials to our problem space (i.e., complex metal oxides are notoriously problematic), and fine tuning the numerical procedure. In an effort to validate theory, we

developed a model system by incremental B-site substitution of a $\text{Sr}(\text{Mn}_x\text{Ce}_{1-x})\text{O}_3$ perovskite.

The data presented in Figures 2a and 2b show the effects of replacing Ce with Mn in SrCeO_3 . In the base perovskite, Ce is trapped in the 4+ state making it extremely difficult to

reduce. We have shown in the past that SrMnO_3 has very high redox capacity (i.e., large area under O_2 curve in Figure 2a), but does not split water (impossible to reoxidize with steam at $\sim 800^\circ\text{C}$). When Mn and Ce mix on the B-site, the material splits water and has a greater redox capacity than CeO_2 . We are currently conducting detailed electronic structure

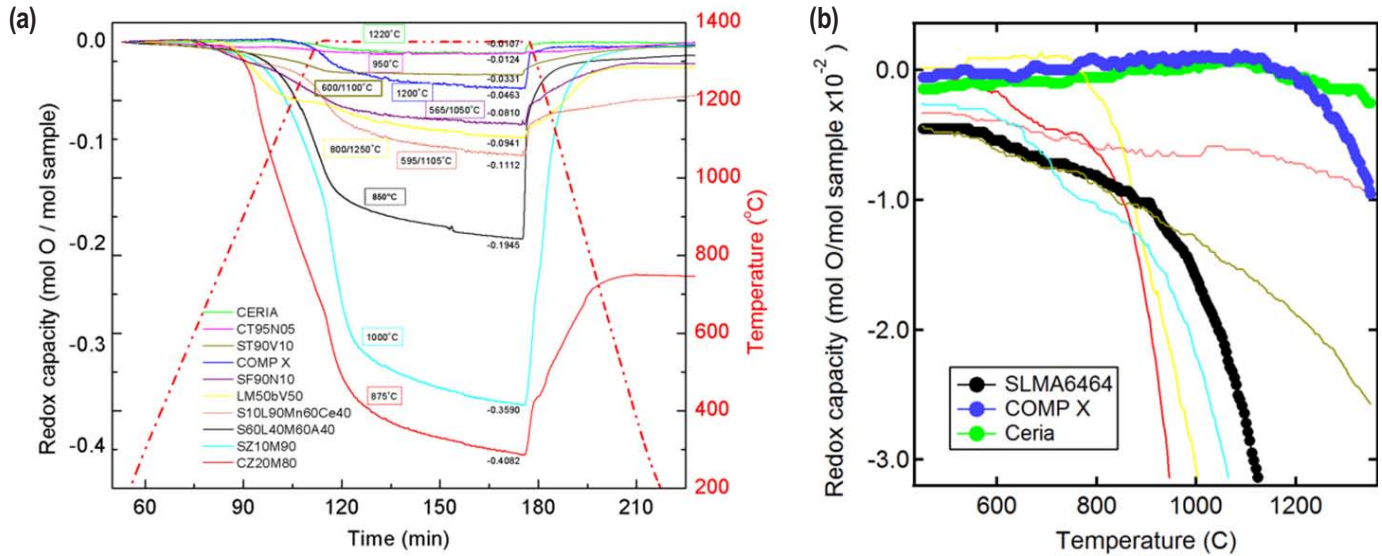


FIGURE 1. (a) Representative mass loss TPR screening results for 10 material formulations obtained using a TGA. Redox capacity is a measure of the mass-normalized moles of O_2 evolved from the sample during the course of heating from room temperature to $1,350^\circ\text{C}$ at $20^\circ\text{C}/\text{min}$, and then dwelling at $1,350^\circ\text{C}$ for 60 min. Temperature values outlined by colored framed boxes shown in graph are the T_{OR} values for each respective compound. (b) Onset temperature for O_2 evolution is derived from the TGA data for SLMA6464 (black), COMPOUND X (blue), and CeO_2 (green). T_{OR} between SLMA6464 and CeO_2 is one positive descriptor for commercially viable redox materials.

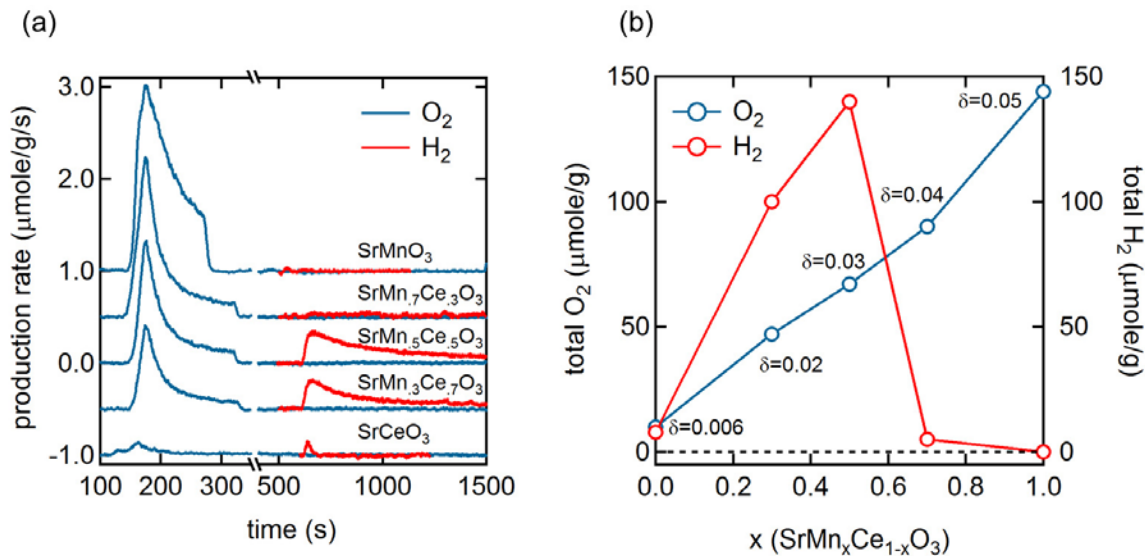


FIGURE 2. (a) O_2 and H_2 production rates for various $\text{SrMn}_x\text{Ce}_{1-x}\text{O}_3$ perovskite formulations measured in Sandia's laser-heated SFR [7]. Thermal reduction is accomplished by heating at $10^\circ\text{C}/\text{s}$ to a T_{RED} in the range $1,200$ – $1,450^\circ\text{C}$. WS conditions were 25%vol H_2O in He at T_{OXD} in the range 850 – $1,000^\circ\text{C}$. The y-axis for each rate curve is offset for clarity. Note that the T_{RED} and T_{OXD} are not the same for all compositions. (b) Representation of the total amount of O_2 and H_2 formed during redox as a function of perovskite composition. The linear correlation with x is coincidental. The data in panels (a) and (b) demonstrates that WS chemistry can be activated/tuned by simple B-site substitution in the SrCeO_3 base perovskite. Understanding this behavior is key to developing optimal materials.

calculations on this system in an effort to validate our DFT approach, and to learn more about tuning perovskite WS activity from an atomistic perspective. Preliminary results of this analysis are encouraging.

CPR2 Design and Testing Thrust

By the conclusion of this project, this team will demonstrate continuous operation of a 3 kW prototype capable of producing >0.5 L/min H₂. In the first nine project months, design work steadily progressed from detailed specification of operating conditions to conceptual layouts of subcomponents, modeling of subcomponent behavior, and to fabrication and testing of certain hardware elements. Key design decisions for the CPR2 were derived during this process, the results of which are briefly summarized in Figure 3.

The solar receiver will consist of two reduction chambers (TR1, TR2) interfaced to pressure separation beds above and below (see Figure 3b). Particle flow will be controlled by gravity and actuation in the downward direction, and by an elevator in the upward direction. In TR1, heat enters through a window and raises the particle temperature to T_{TR} from ~800°C while partially reducing the oxide. In TR2, heat entering the chamber reduces the oxide to its maximum extent. O₂ is removed by pumping. The WS chamber exposes the reduced oxide to steam, in a countercurrent flow

arrangement, to produce H₂ and reoxidize the oxide using a minimum amount of steam. Pressure separation along the flow path is accomplished by low gas permeability through the moving packed particle bed.

Next we describe a few main design challenges, and our solutions to them, associated with specific CPR2 elements.

1. Transferring heat to the oxide particles in TR1 and TR2 quickly and effectively. The small size of the CPR2 prohibits a falling particle approach because the freefall residence time is too short (<0.2 s). We note that this would not be a problem in a large scale system. The particles must therefore be exposed to radiation as a relatively slowly flowing bed, and the results of preliminary heat transfer experiments (see Figure 4a) indicate that the bed depth must be comparable to the particle dimensions. In addition to heat transfer into and within the bed, oxygen flow from a particle undergoing reduction must not be impeded as it makes its way out. To satisfy the above requirements, a thin layer of oxide will be moved through the irradiation zone on a horizontal ceramic plate. The plate will be actuated in a “stick slip” fashion at rates controlled by the operator.

2. Pumping oxygen from TR1 and TR2. Off-the-shelf roughing pumps, namely positive displacement pumps, are suitable but not ideal for the target pressures shown in Figure 3a because, under vacuum, they operate at

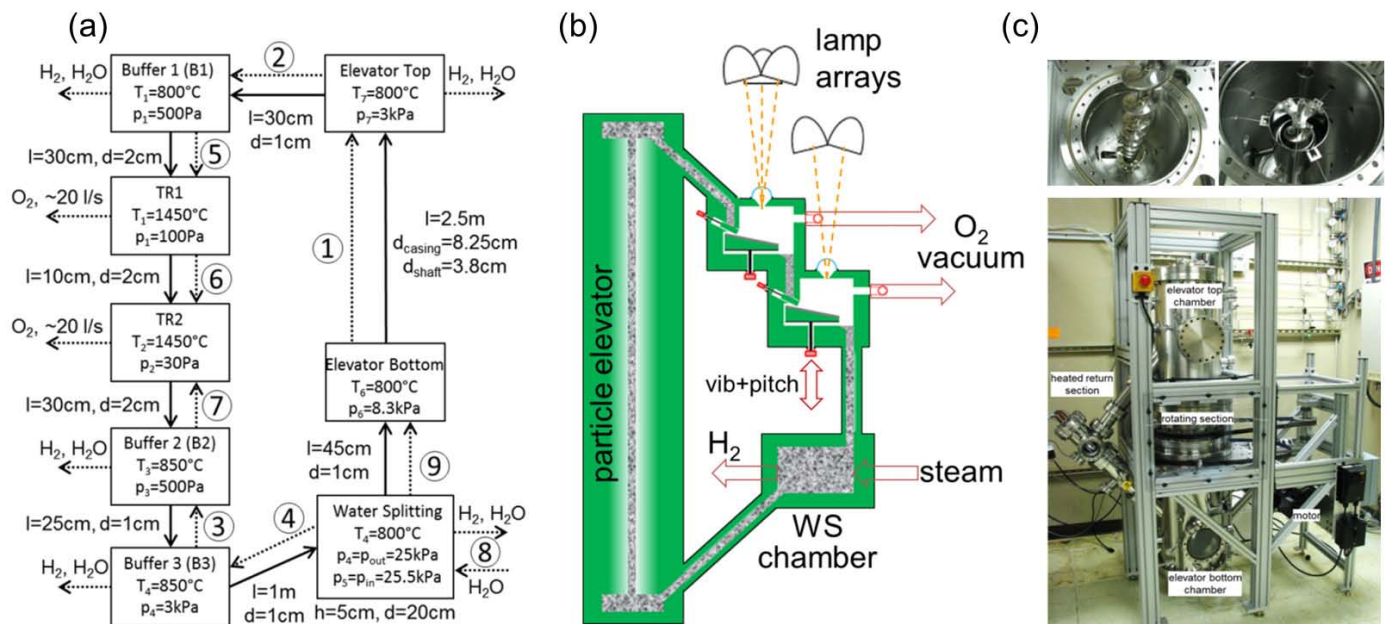


FIGURE 3. (a) CPR2 block diagram loosely resembles reactor geometry. Solid arrows indicate the direction of particle flow in a circular fashion throughout the reactor. Dashed arrows indicate gas flows, from higher to lower pressure elements, also labeled by circled numbers (1–9). Pressures shown are the result of detailed calculations, starting from the nominal input power, and a selection of pump size (pumping speed) for first thermal reduction chamber (TR1). The indicated dimensions (l = length, d = diameter) are those of the internal packed particle beds, not the physical dimensions of the exterior chambers and connecting elements. (b) A conceptual schematic of the CPR2 showing location of packed particle beds, solar lamp arrays, and main chambers. The pressure buffer chambers are not included in the drawing. (c) Picture of the particle elevator that will be incorporated into the CPR2. Top pictures show auger and casing elements as viewed from above.

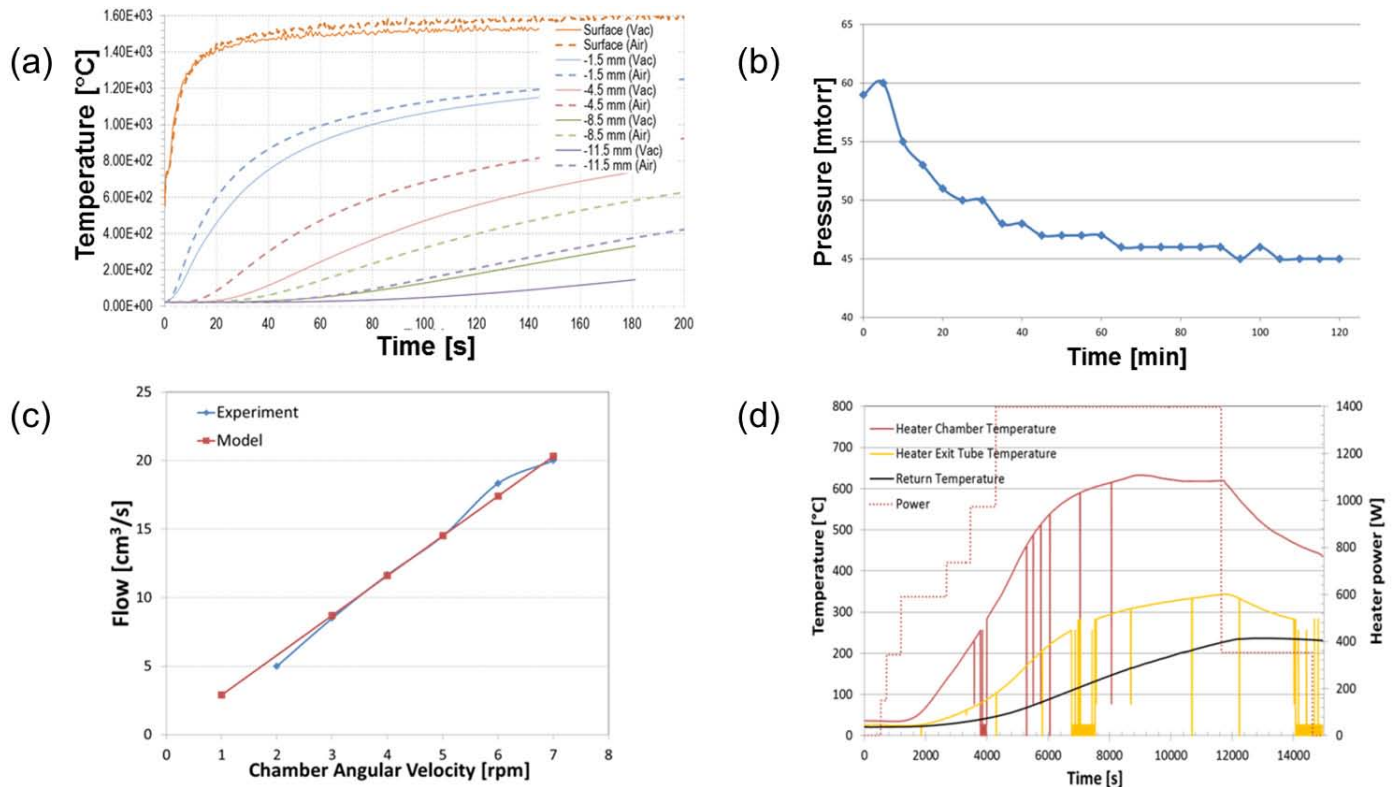


FIGURE 4. (a) Temperature measured in a stagnant bed of particles, as a function of time, during a heating test under solar simulated light in air and in rough vacuum. A pyrometer was used to measure surface temperature, thermocouples were used to measure temperature at indicated heights within the bed from 1.0–11.5 mm below the surface. The results indicate that vacuum and particle shading impede heat transfer to and within the bed. This must be accounted for in the CPR2 design (see text). (b) Pressure measured as a function of time during a room temperature test of the particle elevator pictured in Figure 3c. This result confirms rotary seal operation to be well within design specifications because 45 mtorr vacuum (~6 Pa) is 5x lower than CPR2 requirements (30 Pa). (c) Particle volumetric conveying rate measured as function of chamber angular velocity for particle elevator. Red line corresponds to a model with a conveying efficiency of 0.38. The conveying rate is well above the CPR2 design requirement even at low RPM. (d) Temperature and heater power measured as a function of time during high-temperature operation of the particle elevator at 25 Pa. The test lasted ~6 h, and achieved particle temperatures greater than 600°C. Spikes are due to intermittent gaps in data logging, not actual thermal fluctuations.

relatively low volumetric pumping speeds. Even though our novel cascading pressure design significantly reduces the pumping requirement, performance of existing small positive displacement pumps falls well outside the ideal for this application. Axial flow pumps that provide high flow speeds with modest initial compression are better matched to the CPR2, however, no suitably-sized axial flow pumps are available off the shelf. Therefore, the pumping speeds specified in Figure 3a are a result of compromises and will be accomplished using positive displacement pumps.

3. Ensuring sufficient steam flow throughout WS chamber. Steam must flow at ~0.3 L/s countercurrent to the oxide flow, while not inducing particle bed fluidization. This is a critical design feature of the CPR2, as the H₂O/H₂ ratio is vastly different between countercurrent and mixed flow, with the latter less efficient and requiring much more H₂O for reoxidation. The countercurrent, non-fluidized flow requirement is the main reason to use a large diameter, shallow bed (WS chamber dimensions shown in Figure 3a).

Furthermore, for spherical particles, the ratio of the settling velocity to the minimum fluidization velocity is roughly 50. This ultimately constrains dimensions for all gas-flow chambers and connecting tubes.

4. Particle conveying and pressure separation. Moving particles under vacuum at high temperature is critical to the success of the CPR2. We are using a compact design called an Olds Lift™ to elevate oxidized particles exiting the WS chamber back up to TR1. This device, while inspired by a commercial system, was designed at Sandia to run under vacuum at high temperature. The data in Figures 4b and 4c show test results that confirm our custom built elevator can achieve the required vacuum operation and particle conveyance rate with considerable engineering margin. Preliminary flow test at high temperature, shown in Figure 4d, is also encouraging, especially since this test was conducted without thermal insulation in the elevator. In summary, conveying rates exceed CPR2 requirements by 10x, vacuum requirements by 5x, and we similarly expect

to meet or exceed thermal design requirements in the near future.

Thus far we have incorporated our extensive understanding of this process into the design of a 3 kW-scale reactor. When completed, the CPR2 will be used to evaluate all reactor functions, inclusive of continuous operation and hydrogen production under simulated solar radiation. Data collected from this instrument will be used to further refine reactor designs, and analytically up-scale Sandia's technology to a multi-MW centralized tower system.

CONCLUSIONS AND FUTURE DIRECTIONS

- Continue material discovery and optimization, develop thermodynamic and kinetic models of material performance as needed
- Produce ~100 kg of redox material for full scale CPR2 tests
- Fabricate components, assemble, and test CPR2 on a solar simulator and produce at least 3 liters of H₂ in eight continuous hours of operation
- Build systems models and conduct technoeconomic analysis of a 100 ton H₂/day plant

FY 2015 SELECTED PUBLICATIONS/ PRESENTATIONS

1. Stechel, E.B., Miller, J.E., "Concentrating Solar Thermochemical Fuels: Key Materials Issues for Commercial Viability and Scalability," In *20th International Conference on Solid State Ionics*; Materials Research Society: Keystone, CO, 2015.
2. Shanga, M., Tong, J., Sanders, M., McDaniel, A.H., O'Hayre, R., Chueh, W.C., "Screening Nonstoichiometric Perovskite Oxides for Solar Thermochemical Fuel Production," *submitted to Energy and Environmental Science* **2015**.
3. Muhich, C.L., Weston, K.C., Arifin, D., McDaniel, A.H., Musgrave, C.B., Weimer, A.W., "Extracting Kinetic Information from Complex Gas--Solid Reaction Data," *Industrial Engineering and Chemistry Research* **2015**, *54*, 4113–4122.
4. McDaniel, A., O'Hayre, R., Tong, J., Emery, A., Wolverton, C., "Optimizing Nonstoichiometric Perovskite Oxides for Solar Thermochemical Fuel Production," In *11th International Symposium on Ceramic Materials and Components for Energy and Environmental Applications*; American Ceramics Society: Vancouver, BC, Canada, 2015.
5. McDaniel, A., Ermanoski, I., "Benchmarking a Metal Oxide-Based Thermochemical Cycle for Solar Hydrogen Production," In *227th ECS Meeting*; The Electrochemical Society: Chicago, IL, 2015.
6. Lucero, B., Johnson, N., Stechel, E., McDaniel, A., Ermanoski, I., "Thermodynamic Systems-Level Analysis of Concentrating Solar Tower with Multiple Receivers and Metal Oxide Heat Transfer to Produce Pure Hydrogen," In *9th International Conference on Energy Sustainability*; American Society of Mechanical Engineers: San Diego, CA, 2015.
7. Ermanoski, I., "Maximizing Efficiency in Two-Step Solar-Thermochemical Fuel Production," *Energy Procedia* **2015**, *69*, 1731–1740.
8. Ermanoski, I., "Maximizing Efficiency in Two Step-Solar Thermochemical Fuel Production," In *9th International Conference on Energy Sustainability*; American Society of Mechanical Engineers: San Diego, CA, 2015.
9. Ermanoski, I., "Current and Future Status of Solar-Thermochemical Fuel Technology in the United States," *Journal of the Japan Institute of Energy* **2015**, *94* (3), 189–193.
10. Emery, A.A., Wolverton, C., "Discovery of Novel Perovskites for Solar Thermochemical Water Splitting from High-Throughput First-Principles Calculations," In *20th International Conference on Solid State Ionics*; Materials Research Society: Keystone, CO, 2015.
11. Barcellos, D., Tong, J., Sanders, M., McDaniel, A., O'Hayre, R., "Investigation on Nonstoichiometric Perovskite Oxides of Sr_{1-x}La_xMn_{1-y}Al_yO₃ for Solar Thermochemical Hydrogen Production," In *20th International Conference on Solid State Ionics*; Materials Research Society: Keystone, CO, 2015.
12. Ermanoski, I., "Maximizing Efficiency in Two Step-Solar Thermochemical Fuel Production," In *SolarPaces*; Solar Power and Chemical Energy Systems managed under IEA: Beijing, China, 2014.

REFERENCES

1. N.P. Siegel, J.E. Miller, I. Ermanoski, R.B. Diver, and E.B. Stechel, *Ind. Eng. Chem. Res.*, **52**, 3276–3286 (2013).
2. W.C. Chueh and S.M. Haile, *Philos. Trans. R. Soc. Math. Phys. Eng. Sci.*, **368**, 3269–3294 (2010).
3. R.B. Diver, J.E. Miller, M.D. Allendorf, N.P. Siegel, and R.E. Hogan, *J. Sol. Energy Eng.*, **130**, 041001(1)–041001(8) (2008).
4. A.H. McDaniel, E.C. Miller, D. Arifin, A. Ambrosini, E.N. Coker, R.O'Hayre, W.C. Chueh, and J. Tong, *Energy Environ. Sci.*, **6**, 2424–2428 (2013).
5. J.E. Miller, A.H. McDaniel, and M.D. Allendorf, *Adv. Energy Mater.*, **4**, 1300469 (2014).
6. I. Ermanoski, N.P. Siegel, and E.B. Stechel, *J. Sol. Energy Eng.*, **135**, 031002 (2013).
7. J.R. Scheffe, A.H. McDaniel, M.D. Allendorf, and A.W. Weimer, *Energy Environ. Sci.*, **6**, 963 (2013).